Near-Field ISAC: Beamforming for Multi-Target Detection

Diluka Galappaththige, *Member, IEEE*, Shayan Zargari, Chintha Tellambura, *Fellow, IEEE,*, and Geoffrey Ye Li, *Fellow, IEEE,*

***Abstract*—This article develops multi-target detection in near-field (NF) integrated sensing and communication (ISAC) systems. Specifically, the base station (BS) operates in full-duplex mode to sense the environmental information from the targets while communicating with the users. To minimize BS transmit power and to satisfy communication and sensing rate targets, we design optimal transmit beamforming (for communication and sensing) and reception beamforming at the BS. We develop an iterative beamforming algorithm to solve the resulting non-convex optimization problem. Compared to the traditional far-field benchmark, the proposed NF approach with 255 BS transmit and reception antennas uses $\sim 1118\,\%$ (or $\sim 6\,\mathrm{dBm}$) less BS transmit power to satisfy the required rate requirements. Furthermore, our proposed approach provides precise multi-target location estimates, emphasizing the advantages of NF sensing.**

***Index Terms*—Integrated sensing and communication, Near-field, Beamforming.**

I. Introduction

INTEGRATED sensing and communication (ISAC) is being developed for sixth-generation wireless networks [1]. ISAC systems will utilize ultra-large antenna arrays (i.e., more than 100 antennas) and high frequencies (i.e., $10\,\mathrm{GHz}$ to $10\,\mathrm{THz}$)) for high communication capacity and sensing resolution [1]–[4]. Consequently, propagation characteristics transition from far-field (FF) to near-field (NF) [3], [4].

NF and FF propagation exhibit markedly distinct characteristics. Unlike FF, which propagates with planar waves, NF propagation forms a spherical wavefront. Furthermore, NF fading undergoes more pronounced changes over distance: FF signal strength diminishes with the square of distance, whereas NF signal strength fades with the 4-th to 6-th power of distance. This spherical wave propagation of NF introduces novel possibilities for ISAC [2], [3]. It enables simultaneous distance and angle estimations, reduces communication interference, and minimizes the necessity for distributed arrays and synchronization. The larger array aperture enhances spatial resolution in both angular and range domains. NF's beam-focusing effect enhances the signal-to-noise ratio of echo signals, leading to more precise estimates. In certain sensing applications like human activity recognition, NF's spherical wavefronts may enhance accuracy [2], [3]. Table I compares NF and FF ISAC systems regarding parameter estimation. Specifically, NF's beam-focusing effect and distance estimation aid in detecting targets at the same angle, which is impossible in the FF counterpart [3], [4].

TABLE I: The estimated target parameters in NF and FF ISAC

Parameter	NF	FF
Angle	✓	✓
Distance	✓	✗

Previous NF ISAC research has focused on single-target systems [3]–[6], without treating the multiple-target detection problem. The primary challenge of the latter is mitigating interference between target echo signals. In particular, targets' shapes, sizes, and materials vary, influencing the strength of the echo signal. Thus, echoes from numerous targets interfere with a single target, reducing the signal-to-interference-plus-noise ratio (SINR) and creating target detection ambiguity. Also, the trade-offs between sensing and communication must be balanced in ISAC. Thus, this study offers a beamforming framework that mitigates interference between target echo signals while capturing NF channel characteristics.

To achieve these goals, we utilize a base station (BS) that operates in full-duplex (FD) mode. The FD mode allows the BS to discern echoes from multiple targets (i.e., sensing) while communicating with the users. We aim to reduce the BS's transmit power while ensuring the system's efficacy in handling both sensing and communication tasks. We jointly optimize the transmit and receive beamforming at the BS to achieve this. To handle the resulting optimization problem, we utilize the alternating optimization (AO) method, combined with semi-definite relaxation (SDR) and Rayleigh quotient techniques. We develop a highly efficient solution. For example, our NF system uses approximately $\sim 1118\,\%$ (or $\sim 6\,\mathrm{dBm}$) less transmit power than conventional FF benchmarks for 255 BS transmit and reception antennas. Furthermore, our approach ensures precise multi-target location estimates.

Notation: Vectors (lower-case) and matrices (upper-case) are bold. $\mathbf{A}^{\mathrm{T}}$, $\mathbf{A}^{\mathrm{H}}$, $\mathrm{Tr}(\mathbf{A})$, and $\mathrm{diag}(\mathbf{A})$ denote transpose, Hermitian transpose, trace, and diagonal operator. $\mathbf{I}_M$ is the $M \times M$ identity matrix. $\|\cdot\|$, $\mathbb{E}[\cdot]$, and $|\cdot|$ denote the Euclidean norm, expectation, and absolute value. $\mathcal{CN}(\boldsymbol{\mu}, \mathbf{R})$ is a complex Gaussian vector with mean $\boldsymbol{\mu}$ and co-variance $\mathbf{R}$. If $f(x) = \mathcal{O}(g(x))$, there exists M and a such that $f(x) \leq Mg(x)$ for all $x \geq a$. Finally, $\mathcal{M} \triangleq \{1, \ldots, M\}$, $\mathcal{K} \triangleq \{1, \ldots, K\}$, $\mathcal{L} \triangleq \{1, \ldots, L\}$, $\mathcal{K}_k \triangleq \mathcal{K} \setminus \{k\}$, and $\mathcal{L}_l \triangleq \mathcal{L} \setminus \{l\}$.

II. System Model and Preliminaries

Here, we describe the system model, channel model, and transmission signals in detail.

D. Galappaththige, S. Zargari, and C. Tellambura are with the Department of Electrical and Computer Engineering, University of Alberta, Edmonton, AB, T6G 1H9, Canada (e-mail: {diluka.lg, zargari, ct4}@ualberta.ca).

G. Y. Li is with the ITP Lab, the Department of Electrical and Electronic Engineering, Imperial College London, SW7 2BX London, U.K.(e-mail: geoffrey.li@imperial.ac.uk).

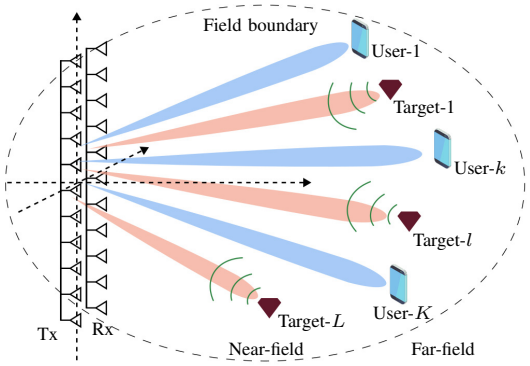

Fig. 1: A NF ISAC system.

A. System Model

We consider a narrowband NF ISAC system having an FD BS with M-transmit and N-receiver antennas, $K \geq 1$ single-antenna communication users, and $L \geq 1$ sensing targets – Fig. 1. Without loss of generality, we assume that the BS antenna arrays are uniform linear arrays (ULAs) with antenna spacing of d and the coordinate system's origin at the center of the ULAs [1]. Thus, the aperture of the transmit (receiver) ULA is $D = (M-1)d$ (or $D = (N-1)d$), resulting in Rayleigh distance of $2D^2/\lambda$, which defines the boundary between NF and FF. In addition, λ is the signal wavelength [4]. We further assume that the users and sensing targets are in the BS's NF region, i.e., the Fresnel region of NF, $1.2D \leq r \leq 2D^2/\lambda$, where r is the user/target distance from the BS [4].

B. Channel Model

We employ the NF spherical wave channel model for the channels between the BS and user/targets [4], [7]. We denote the channel between the transmit ULA and the k-th user and the transmit ULA and the l-th target as $\mathbf{h}_k \in \mathbb{C}^{M\times 1}$ and $\mathbf{g}_{f,l} \in \mathbb{C}^{M\times 1}$, respectively, while $\mathbf{g}_{b,l} \in \mathbb{C}^{N\times 1}$ represents the channel between the l-th target and the BS receiver ULA.

The coordinate of the m-th element of transmit ULA is given as $\mathbf{s}_m = [0, md]$ for $m \in \mathcal{M}$. Let the k-th user be located at r_k distance and θ_k angle from the center of the transmit ULA. The k-th user coordinate is thus given as $\mathbf{v}_k = [r_k\cos(\theta_k), r_k\sin(\theta_k)]$. The distance from the m-th transmit antenna element to the k-th user is calculated as

$$r_{mk} = \|\mathbf{v}_k - \mathbf{s}_m\| = \sqrt{r_k^2 + m^2d^2 - 2mdr_k\sin(\theta_k)}. \quad (1)$$

Therefore, the channel between the m-th transmit antenna element and the k-th user is given by [4], [7]

$$h_{mk} = \sqrt{\zeta_{mk}}e^{-j\frac{2\pi}{\lambda}r_{mk}}, \quad (2)$$

where ζ_{mk} accounts for the path-loss. The NF channel vector between the BS transmit ULA and the k-th user, $\mathbf{h}_k$, thus can be expressed as

$$\mathbf{h}_k = \left[h_{\frac{-M+1}{2}k}, \ldots, h_{0k}, \ldots h_{\frac{M-1}{2}k}\right]^{\mathrm{T}} = \boldsymbol{\zeta}_k^{1/2}\mathbf{a}_h(r_k,\theta_k), \quad (3)$$

where $\boldsymbol{\zeta}_k = \mathrm{diag}(\zeta_{\frac{-M+1}{2}\mathrm{k}}, \ldots, \zeta_{\frac{M-1}{2}\mathrm{k}})$ and $\mathbf{a}_h(r_k,\theta_k)$ is the NF array response vector with $[\mathbf{a}_h(r_k,\theta_k)]_m = e^{-j\frac{2\pi}{\lambda}r_{mk}}$.

[1]Note that the transmit and receive ULAs may be separated by placing them in the z-axis for self-interference (SI) cancellation.

Finally, $\mathbf{G}_{\mathrm{SI}} \in \mathbb{C}^{M\times N}$ represents the SI channel between the transmitter and the receiver antennas of the BS.

We assume the use of distinct time slots for channel estimation and data transmission/sensing, i.e., time-division duplexing. Thus, a one-time slot in each coherent interval is reserved for estimating channel state information (CSI), which can be done via emerging methods [8]. Thus, we assume the availability of perfect CSI. This assumption is standard and yields upper-bound performance limits.

C. Transmission Signal

The BS transmits signal $\mathbf{x}$ to communicate with users and sense targets, i.e., $\mathbf{x} = \sum_{i\in\mathcal{K}}\mathbf{w}_i q_i + \sum_{j\in\mathcal{L}}\mathbf{s}_j$, where $q_i \in \mathbb{C}$ is the intended data symbol for the i-th user with unit power, i.e., $\mathbb{E}\{|q_i|^2\} = 1$, $\mathbf{w}_i \in \mathbb{C}^{M\times 1}$ is the BS data beamforming vector for the i-th user, and $\mathbf{s}_j \in \mathbb{C}^{M\times 1}$ is the sensing signal for the j-th target with the covariance matrix $\mathbf{S}_j \triangleq \mathbb{E}\{\mathbf{s}_j\mathbf{s}_j^{\mathrm{H}}\}$. Here, it is assumed that q_i and $\mathbf{s}_j$ are independent of each other, and the beamforming at the BS is achieved through designing $\mathbf{w}_i$ and $\mathbf{S}_j$ [9]. The received signal at the k-th user is given by

$$\begin{aligned} y_k &= \mathbf{h}_k^{\mathrm{H}}\mathbf{x} + z_k \\ &= \mathbf{h}_k^{\mathrm{H}}\mathbf{w}_k q_k + \sum\nolimits_{i\in\mathcal{K}_k}\mathbf{h}_k^{\mathrm{H}}\mathbf{w}_i q_i + \sum\nolimits_{j\in\mathcal{L}}\mathbf{h}_k^{\mathrm{H}}\mathbf{s}_j + z_k, \end{aligned} \quad (4)$$

where $z_k \sim \mathcal{CN}(0,\sigma^2)$ is the k-th user white Gaussian noise (AWGN) with 0 mean and σ^2 variance.

Meanwhile, the targets reflect $\mathbf{x}$, which comes back to the receiver at the BS. This received signal is given as

$$\mathbf{y}_b = \sum\nolimits_{j\in\mathcal{L}}\sqrt{\alpha_j}\mathbf{g}_{b,j}\mathbf{g}_{f,j}^{\mathrm{H}}\mathbf{x} + \mathbf{G}_{\mathrm{SI}}\mathbf{x} + \mathbf{z}_b, \quad (5)$$

where α_j is the j-th target power reflection coefficient, $\mathbf{G}_{\mathrm{SI}}\mathbf{x}$ represents the SI at the receiver of the BS due to simultaneous transmission and reception, and $\mathbf{z}_b \sim \mathcal{CN}(\mathbf{0},\sigma^2\mathbf{I}_N)$ is the AWGN at the BS. Due to the limited dynamic range of the receiver, SI cannot be canceled perfectly even with the perfect CSI of the SI channel [10]. After the SI cancellation, the BS applies the receiver beamforming, $\mathbf{u}_l$ for $l \in \mathcal{L}$, to the received signal (5) to acquire the desired reflected signal of the l-th target. The post-processed SI cancelled signal is thus given as

$$\begin{aligned} y_{b,l} = \sqrt{\alpha_l}\mathbf{u}_l^{\mathrm{H}}\mathbf{G}_l\mathbf{x} + \sum\nolimits_{j\in\mathcal{L}_l}\sqrt{\alpha_j}\mathbf{u}_l^{\mathrm{H}}\mathbf{G}_j\mathbf{x} \\ + \sqrt{\beta}\mathbf{u}_l^{\mathrm{H}}\mathbf{G}_{\mathrm{SI}}\mathbf{x} + \mathbf{u}_l^{\mathrm{H}}\mathbf{z}_b, \end{aligned} \quad (6)$$

where $\mathbf{G}_j \triangleq \mathbf{g}_{b,j}\mathbf{g}_{f,j}^{\mathrm{H}}$ and $0 < \beta \ll 1$ accounts for the SI cancellation quality.

SI cancellation in conventional FD radios involves hardware techniques, analog domain cancellation, and digital domain cancellation of residual SI [10]. These can also be developed for ISAC systems.

D. Communication and Sensing Rates

The critical system measures include the attainable rate at the users and the sensing rate at the BS. Hence, we develop computational formulas for these.

From (4), the received SINR at the k-th user can be written as

$$\gamma_k = \frac{|\mathbf{h}_k^{\mathrm{H}}\mathbf{w}_k|^2}{\sum_{i\in\mathcal{K}_k}|\mathbf{h}_k^{\mathrm{H}}\mathbf{w}_i|^2 + \sum_{j\in\mathcal{L}}\mathbf{h}_k^{\mathrm{H}}\mathbf{S}_j\mathbf{h}_k + \sigma^2}. \quad (7)$$

Thereby, the rate of the k-th user is approximately given as

$$\mathcal{R}_{c,k} = \log_2(1+\gamma_k). \tag{8}$$

The BS uses the target's reflected signal to detect and extract environmental information. To this end, using (6), the sensing rate of the l-th target at the BS is approximately given as [9]

$$\mathcal{R}_{s,l} \approx \log_2(1+\Gamma_l), \tag{9}$$

where Γ_l is the l-th target sensing SINR and given as

$$\begin{aligned}\Gamma_l &= \frac{\alpha_l \mathbb{E}\{|\mathbf{u}_l^{\mathrm{H}}\mathbf{G}_l\mathbf{x}|^2\}}{\sum\limits_{j\in\mathcal{L}_l}\alpha_j\mathbb{E}\{|\mathbf{u}_l^{\mathrm{H}}\mathbf{G}_j\mathbf{x}|^2\}+\beta\mathbb{E}\{|\mathbf{u}_l^{\mathrm{H}}\mathbf{G}_{\mathrm{SI}}\mathbf{x}|^2\}+\mathbb{E}\{|\mathbf{u}_l^{\mathrm{H}}\mathbf{z}_b|^2\}} \\ &= \frac{\alpha_l \mathbf{u}_l^{\mathrm{H}}\mathbf{G}_l\mathbf{R}_x\mathbf{G}_l^{\mathrm{H}}\mathbf{u}_l}{\mathbf{u}_l^{\mathrm{H}}\left(\sum\limits_{j\in\mathcal{L}_l}\alpha_j\mathbf{G}_j\mathbf{R}_x\mathbf{G}_j^{\mathrm{H}}+\beta\mathbf{G}_{\mathrm{SI}}\mathbf{R}_x\mathbf{G}_{\mathrm{SI}}^{\mathrm{H}}+\sigma^2\mathbf{I}_N\right)\mathbf{u}_l},\end{aligned} \tag{10}$$

where $\mathbf{R}_x \triangleq \mathbb{E}\{\mathbf{x}\mathbf{x}^{\mathrm{H}}\} = \sum_{i\in\mathcal{K}}\mathbf{w}_i\mathbf{w}_i^{\mathrm{H}} + \sum_{j\in\mathcal{L}}\mathbf{S}_j$ is the variance matrix of the BS transmitted signal [9].

Remark 1. *The sensing rate indicates how much environmental information can be extracted from the reflected signal of a particular target. It may also be useful for optimal sensing waveform designs [11]. In addition, the sensing rate can be useful for transmit and receive beamforming design for target detection [9]. In contrast, the standard transmit-beampattern's mean squared error does not account for the receiver beam pattern or target interference.*

III. Problem Formulation

Herein, we aim to minimize the transmit power at the BS to reduce the system's power consumption. In particular, we optimize the BS's transmit beamforming, $\{\mathbf{w}_k\}_{k\in\mathcal{K}}$ and $\{\mathbf{S}_l\}_{l\in\mathcal{L}}$, and the receiver beamforming, $\{\mathbf{u}_l\}_{l\in\mathcal{L}}$, while maintaining the communication and sensing rate demands at users and the BS, respectively. This goal fosters large-scale connectivity by reusing saved power to expand network capacity for more users and targets. This method is especially advantageous for green Internet-of-Things (IoT) networks, which aim to reduce energy usage. On the other hand, our study tackles the distinct challenges of power minimization in NF ISAC systems, where targets actively contribute to the sensing process. Unlike traditional setups, such as cognitive radio systems focused on interference, NF ISAC strives to balance communication efficiency and sensing accuracy.

Defining $\mathcal{A} = \{\{\mathbf{u}_l\}_{l\in\mathcal{L}}, \{\mathbf{w}_k\}_{k\in\mathcal{K}}, \{\mathbf{S}_l \succ 0\}_{l\in\mathcal{L}}\}$ as optimization variables, the formulated problem is thus given by

$$\mathbf{P}: \min_{\mathcal{A}} \quad \sum\nolimits_{k\in\mathcal{K}}\|\mathbf{w}_k\|^2 + \sum\nolimits_{l\in\mathcal{L}}\mathrm{Tr}(\mathbf{S}_l), \tag{11a}$$

$$\text{s.t. } \gamma_k \geq \gamma_k^{\mathrm{th}}, \quad \forall k, \tag{11b}$$

$$\Gamma_l \geq \Gamma_l^{\mathrm{th}}, \quad \forall l, \tag{11c}$$

$$\|\mathbf{u}_l\|^2 = 1, \quad \forall l, \tag{11d}$$

where (11b) and (11c) guarantee the required communication and sensing rates at users and the BS, respectively. Note that since the user/tag communication/sensing rates are monotonically increasing functions of their arguments, i.e., SINR, we replace rates with respective SINRs to obtain constraints (11b) and (11c). Thus, $\gamma_k^{\mathrm{th}} \triangleq 2^{\mathcal{R}_{c,k}^{\mathrm{th}}} - 1$ and $\Gamma_l^{\mathrm{th}} \triangleq 2^{\mathcal{R}_{s,l}^{\mathrm{th}}} - 1$ with $\mathcal{R}_{c,k}^{\mathrm{th}}$ and $\mathcal{R}_{s,l}^{\mathrm{th}}$ denote the respective targeted communication and sensing rates. Constraint (11d) is the reception filter's normalization constraint at the BS.

IV. Proposed Solution

Due to the involved products of the optimization variables, problem $\mathbf{P}$ is non-convex. Thus, we decompose $\mathbf{P}$ into two sub-problems [12]. This AO approach iteratively optimizes a variable or set of variables while keeping the rest of the variables fixed until convergence is achieved.

A. Sub-problem 1: Receiver beamforming optimization

With fixed transmit beamformers, $\{\mathbf{w}_k\}_{k\in\mathcal{K}}$ and $\{\mathbf{S}_l\}_{l\in\mathcal{L}}$, the receiver beamforming, $\{\mathbf{u}_l\}_{l\in\mathcal{L}}$, becomes a variable in a feasibility problem, where it does not directly affect BS transmit power minimization. To support the indirect aim of power reduction, $\mathbf{u}_l$ is optimized to enhance the sensing SINR of each target. This method leverages the sensing SINR's structure, transforming the sub-problem into a generalized Rayleigh quotient problem with a known closed-form solution [13]. Thus, we have the following optimization problem:

$$\mathbf{P}_{\mathrm{u}}: \max_{\mathbf{u}_l} \quad \frac{\alpha_l \mathbf{u}_l^{\mathrm{H}}\mathbf{G}_l\mathbf{R}_x\mathbf{G}_l^{\mathrm{H}}\mathbf{u}_l}{\mathbf{u}_l^{\mathrm{H}}\left(\sum\limits_{j\in\mathcal{L}_l}\alpha_j\mathbf{G}_j\mathbf{R}_x\mathbf{G}_j^{\mathrm{H}}+\beta\mathbf{G}_{\mathrm{SI}}\mathbf{R}_x\mathbf{G}_{\mathrm{SI}}^{\mathrm{H}}+\sigma^2\mathbf{I}_N\right)\mathbf{u}_l}, \tag{12a}$$

$$\text{s.t. } \|\mathbf{u}_l\|^2 = 1, \quad \forall l, \tag{12b}$$

The objective function in (12a) can be restated as the following optimization problem

$$\mathbf{P}_{\mathrm{u1}}: \max_{\mathbf{u}_l} \quad \mathbf{u}_l^{\mathrm{H}}\tilde{\mathbf{g}}_l\tilde{\mathbf{g}}_l^{\mathrm{H}}\mathbf{u}_l / \mathbf{u}_l^{\mathrm{H}}\mathbf{Q}_l\mathbf{u}_l, \tag{13a}$$

$$\text{s.t. (12b)}, \tag{13b}$$

where $\tilde{\mathbf{g}}_l = \sqrt{\alpha_l}\mathbf{G}_l\left(\sum_{i\in\mathcal{K}}\mathbf{w}_i + \sum_{j\in\mathcal{L}}\mathbf{s}_j\right)$ and $\mathbf{Q}_l = \sum_{j\in\mathcal{L}_l}\alpha_j\mathbf{G}_j\mathbf{R}_x\mathbf{G}_j^{\mathrm{H}} + \beta\mathbf{G}_{\mathrm{SI}}\mathbf{R}_x\mathbf{G}_{\mathrm{SI}}^{\mathrm{H}} + \sigma^2\mathbf{I}_N$. Problem $\mathbf{P}_{\mathrm{u1}}$ is a generalized Rayleigh ratio quotient problem. The optimal received beamformer is thus given by

$$\mathbf{u}_l^* = \mathbf{Q}_l^{-1}\tilde{\mathbf{g}}_l / \|\mathbf{Q}_l^{-1}\tilde{\mathbf{g}}_l\|, \quad \forall l, \tag{14}$$

which is a minimal mean-squared error (MMSE) filter [13].

B. Sub-problem 2: Transmit beamforming optimization

For a given received beamforming, $\{\mathbf{u}_l\}_{l\in\mathcal{L}}$, problem $\mathbf{P}$ resembles a transmit beamforming optimization problem. We first define the matrix $\mathbf{W}_k \triangleq \mathbf{w}_k\mathbf{w}_k^{\mathrm{H}}$, where $\mathbf{W}_k$ is a semi-definite matrix with a rank one constraint, i.e., $\mathrm{Rank}(\mathbf{W}_k) = 1$. By utilizing SDR techniques to relax the highly non-convex rank one constraints, the resultant problem is formulated as

$$\mathbf{P}_{\mathrm{w}}: \min_{\mathbf{W}_k,\mathbf{S}_l} \sum\nolimits_{k\in\mathcal{K}}\mathrm{Tr}(\mathbf{W}_k) + \sum\nolimits_{l\in\mathcal{L}}\mathrm{Tr}(\mathbf{S}_l), \tag{15a}$$

$$\text{s.t.} \sum\nolimits_{i\in\mathcal{K}_k}\mathrm{Tr}(\mathbf{h}_k\mathbf{h}_k^{\mathrm{H}}\mathbf{W}_i) + \sum\nolimits_{j\in\mathcal{L}}\mathrm{Tr}(\mathbf{h}_k\mathbf{h}_k^{\mathrm{H}}\mathbf{S}_j) + \sigma^2 - \mathrm{Tr}(\mathbf{h}_k\mathbf{h}_k^{\mathrm{H}}\mathbf{W}_k)/\gamma_k^{\mathrm{th}} \leq 0, \quad \forall k, \tag{15b}$$

Algorithm 1 : Iterative Beamforming Algorithm

1: **Input**: Set the iteration counter $t = 0$, the convergence tolerance $\epsilon > 0$, initial feasible solution $\{\mathbf{w}_k\}_{k\in\mathcal{K}}$ and $\{\mathbf{S}_l\}_{l\in\mathcal{L}}$. Initialize the objective function value $F^{(0)} = 0$.
2: **while** $\frac{F^{(t+1)}-F^{(t)}}{F^{(t+1)}} \geq \epsilon$ **do**
3: Solve (14) for the received beamformer, $\mathbf{u}_k^{(t+1)}$.
4: Solve (15) to obtain transmit beamformers by recovering a rank-one solution via GR, $\{\mathbf{w}_k^{(t+1)}, \mathbf{s}_l^{(t+1)}\}$.
5: Calculate the objective function value $F^{(t+1)}$.
6: Set $t \leftarrow t + 1$;
7: **end while**
8: **Output**: Optimal solutions $\mathcal{A}^*$.

$$\sum_{j\in\mathcal{L}_l}\alpha_j\left(\sum_{i\in\mathcal{K}}\text{Tr}(\mathbf{g}_j\mathbf{g}_j^{\text{H}}\mathbf{W}_i)+\sum_{q\in\mathcal{L}}\text{Tr}(\mathbf{g}_j\mathbf{g}_j^{\text{H}}\mathbf{S}_q)\right)+\frac{\|\mathbf{u}_l\|^2}{\sigma^{-2}}$$
$$+\beta\left(\sum_{i\in\mathcal{K}}\text{Tr}(\mathbf{g}_{\text{SI},j}\mathbf{g}_{\text{SI},j}^{\text{H}}\mathbf{W}_i)+\sum_{q\in\mathcal{L}}\text{Tr}(\mathbf{g}_{\text{SI},j}\mathbf{g}_{\text{SI},j}^{\text{H}}\mathbf{S}_q)\right)$$
$$-\frac{\alpha_l}{\Gamma_l^{\text{th}}}\left(\sum_{i\in\mathcal{K}}\text{Tr}(\mathbf{g}_l\mathbf{g}_l^{\text{H}}\mathbf{W}_i)+\sum_{q\in\mathcal{L}}\text{Tr}(\mathbf{g}_l\mathbf{g}_l^{\text{H}}\mathbf{S}_q)\right)\leq 0,\ \forall l, \text{(15c)}$$

where $\mathbf{g}_j \triangleq \mathbf{G}_j^{\text{H}}\mathbf{u}_l$ and $\mathbf{g}_{\text{SI},j} \triangleq \mathbf{G}_{\text{SI}}^{\text{H}}\mathbf{u}_l$. The rank-1 relaxed $\mathbf{P}_{\text{w}}$ can be solved as a standard semi-definite programming (SDP) problem and CVX Matlab tool.

The optimal solution of $\mathbf{P}_{\text{w}}$, denoted by $\mathbf{W}_k^*$, is not necessarily rank-1. However, if it is, the only eigenvalue is the trace of $\mathbf{W}_k^*$; the corresponding eigenvector determines the optimal beamforming vector. Otherwise, we need to extract a rank-1 solution from $\mathbf{W}_k^*$. To do that, we can pick a random vector $\mathbf{r}$ from $\mathcal{CN}(0, \mathbf{W}_k^*)$ and then project it to the feasible region of $\mathbf{P}_{\text{w}}$. This random sampling is performed 10^3 times, and we pick only the best approximate solution. This approach is known as Gaussian randomization (GR) [14].

All these steps are put together in Algorithm 1. It begins with the initialization of $\{\mathbf{w}_k\}_{k\in\mathcal{K}}$ and $\{\mathbf{s}_l\}_{l\in\mathcal{L}}$ to random but feasible values. In each iteration, it refines the values of $\{\{\mathbf{w}_k\}_{k\in\mathcal{K}}, \{\mathbf{s}_l\}_{l\in\mathcal{L}}, \{\mathbf{u}_l\}_{l\in\mathcal{L}}\}$ until the normalized improvement of the objective is smaller than $\epsilon = 10^{-3}$.

Remark 2. *Within the AO framework, each sub-problem is structured for local optimality, with convergence to a local minimum ensured under specific conditions, such as lower-boundedness and smoothness of the objective function [12]. The SDR method address the sub-problem for $\{\{\mathbf{w}_k\}_{k\in\mathcal{K}}, \{\mathbf{s}_l\}_{l\in\mathcal{L}}\}$ while $\{\mathbf{u}_l\}_{l\in\mathcal{L}}$ is derived directly via the Rayleigh quotient. As the SDR method is a well-established optimization technique with provable convergence, the convergence of our AO approach is underpinned, ensuring its reliability and efficacy [14]. Nonetheless, our simulation results also corroborate the validity of this claim (Fig. 2).*

C. Computational Complexity

The computational complexity of Algorithm 1 mainly depends on the SDR and Rayleigh quotient techniques. The optimal received beamforming is obtained using the Rayleigh quotient. Computing the inverse of the matrix $\mathbf{Q}_l$ requires $\mathcal{O}(N^3)$. Additionally, the MMSE filter for the L targets adds $\mathcal{O}(LN^2)$ complexity. Therefore, the complexity is $\mathcal{O}(LN^2 + N^3)$. Sub-problem 2 based on the SDP is solved via the interior-point method. From [15, Th. 3.12], the complexity of a SDP problem with m SDP constraints, which includes a $n \times n$ positive semi-definite (PSD) matrix, is $\mathcal{O}\left(\sqrt{n}\log\left(\frac{1}{\epsilon}\right)(mn^3 + m^2n^2 + m^3)\right)$, where $\epsilon > 0$ is the solution accuracy. With $n = M$ and $m = K + L$, the approximate computational complexity for solving $\mathbf{P}_{\text{w}}$ can be given as $\mathcal{O}\left((K + L)M^3\sqrt{M}\log\left(\frac{1}{\epsilon}\right)\right)$.

TABLE II: Simulation parameters.

Parameter	Value	Parameter	Value
f_c	28 GHz	K_0	27.5
d	$\lambda/2$	σ^2	-100 dBm
K	3	β	-60 dB
L	2	$\mathcal{R}_{c,l}^{\text{th}}$	10 bps/Hz
η	2	$\mathcal{R}_{s,l}^{\text{th}}$	5 bps/Hz

V. Simulation Results

In this section, we present simulation results for assessing the performance of the NF ISAC system with multiple targets. We use the free-space path-loss model for the large-scale fading as $\zeta_{mk} = K_0 + \eta\log_{10}(r_{mk})$, where K_0 is the path loss at the reference distance $d_0 = 1$ m and η is the path-loss exponent. The users and the targets are randomly distributed within an area having an inner radius of 40 m and an outer radius of 50 m, i.e., $\{r_k, r_l\} \sim U(40, 50)$ and $\{\theta_k, \theta_l\} \sim U(-\pi/2, \pi/2)$. Unless otherwise specified, Table II summarizes the simulation parameters. All simulation is evaluated for 10^3 iterations. We compare the following benchmarks against the proposed NF ISAC system.

1) *FF ISAC:* Since $D \ll r_k$ in the FF, the channel response in (2) becomes $h_{mk} = \sqrt{\zeta_k}e^{j\frac{2\pi}{\lambda}md\sin(\theta_k)}$ [4], [7]. This benchmark aids in determining the cost of inadequate channel modeling in NF ISAC.
2) *Communication-only:* This evaluates the system's communication capabilities primarily through multi-user communication, i.e., $\mathbf{x} = \sum_{k\in\mathcal{K}}\mathbf{w}_k q_k$.
3) *Sensing-only:* This focuses on a sensing-centric system with multi-targets, i.e., $\mathbf{x} = \sum_{l\in\mathcal{K}}\mathbf{s}_l$.

Fig. 2 depicts the convergence behavior of Algorithm 1 for different combinations of K and L with $M = N = 255$. The objective is to minimize the BS transmit power while satisfying communication and sensing rates at the users and the BS, respectively. Algorithm 1 outputs optimal $\{\mathbf{u}_l\}_{l\in\mathcal{L}}$, $\{\mathbf{w}_k\}_{k\in\mathcal{K}}$, and $\{\mathbf{s}_l\}_{l\in\mathcal{L}}$, for a given NF ISAC system setup. The BS power stabilizes after several iterations and shows convergence. As per Fig. 2, the objective decreases rapidly and saturates as the number of iterations grows. Specifically, regardless of M, K, or L, the overall algorithm converges in less than 5 iterations.

Fig. 3 explores the effect of the number of BS antennas, $M = N$, on the BS transmit power for $K = 3$ and $L = 2$. A clear and continuous trend emerges in BS transmit power (Fig. 3); increasing the number of BS transmit antennas has

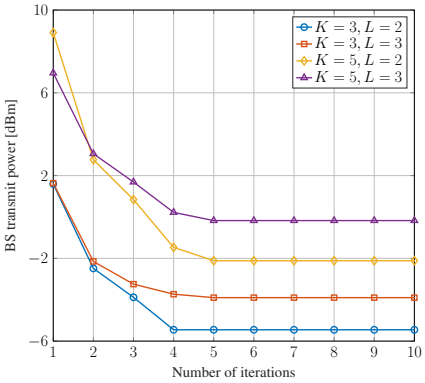

Fig. 2: Convergence of the proposed Algorithm 1 for $M = N = 255$.

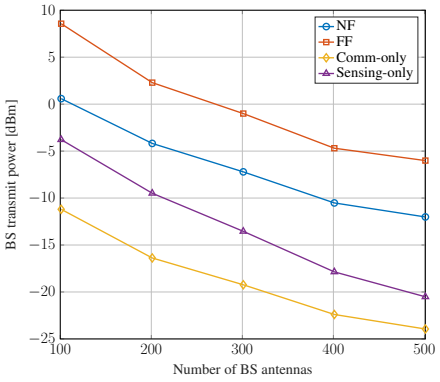

Fig. 3: Transmit power versus the number of antennas at the BS, $M = N$.

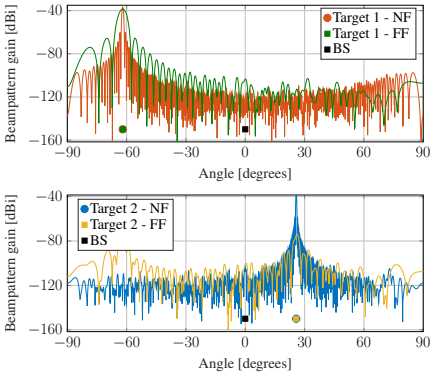

Fig. 4: Beampattern of radar functionality of Algorithm 1 with NF and FF channels for $M = N = 255$.

an inverse influence on the necessary power. An increase in antenna count, in particular, decreases transmission power across all the schemes. This is because of their singular focus on communication or sensing tasks, which allows them to allocate transmit power more effectively to their primary goal. In contrast, the FF system has the worst transmit power performance due to distributed beam energy and multi-user/target interference. Conversely, the NF system performs better as it can handle user interference at the same angle. For example, with $M = N = 255$, the NF system requires a $\sim 1118\,\%$ (or $\sim 6\,\mathrm{dBm}$) lower transmit power than the FF system to meet the required communication and sensing rates.

Fig. 4 illustrates the radar functionality of Algorithm 1 to direct the transmit and receiver beams in specific directions. The algorithm converges signals from an array of antennas, crafting a directed "beam" or "lobe" [9], [16]. The beam is electronically steered while the antennas remain stationary. This capability amplifies signal quality, boosts target detection, and significantly minimizes potential interference [9], [16].

Conversely, the transmit signal, representing the outward-projected energy, is critical in efficiently illuminating the targets. Meanwhile, the received beamforming is optimized for clear reception, capturing the echoes or reflections off the targets. To this end, the beampattern gain is defined as $p(\theta_l) = |(\mathbf{u}_l^*)^{\mathrm{H}}\mathbf{g}_{b,l}\mathbf{g}_{f,l}^{\mathrm{H}}\mathbf{x}^*|^2$. Fig. 4 depicts the beampattern gain generated by Algorithm 1 for NF and FF ISAC systems. As shown in Fig. 4, our proposed NF beamforming design has higher power at target locations than the FF counter design, indicating that the beam of the NF beamforming design has superior target estimated performance in ISAC systems

VI. Conclusion

This article investigates a multi-target, multi-user ISAC network. The FD BS detects echoes from the targets while communicating with the users. We minimize the BS power consumption via transmit and receiver beamforming optimization while guaranteeing the required communication and sensing rates. The problem is nonconvex; thus, we combined AO, SDR, and Rayleigh quotient techniques. The resulting algorithm offers precise multi-target location estimation, promoting the benefits of NF sensing. Future directions include machine learning algorithms, energy efficiency, interference control, and integration with 6G.

References

[1] F. Liu *et al.*, "Integrated sensing and communications: Toward dual-functional wireless networks for 6G and beyond," *IEEE J. Sel. Areas Commun.*, vol. 40, no. 6, pp. 1728–1767, Jun. 2022.

[2] H. Zhang *et al.*, "Beam focusing for near-field multiuser MIMO communications," *IEEE Trans. Wireless Commun.*, vol. 21, no. 9, pp. 7476–7490, Sept. 2022.

[3] K. Qu, S. Guo, and N. Saeed, "Near-field integrated sensing and communication: Performance analysis and beamforming design," *arXiv*, 2023.

[4] Z. Wang, X. Mu, and Y. Liu, "Near-field integrated sensing and communications," *IEEE Commun. Lett.*, vol. 27, no. 8, pp. 2048–2052, Aug. 2023.

[5] B. Zhao, C. Ouyang, Y. Liu, X. Zhang, and H. V. Poor, "Modeling and analysis of near-field ISAC," *arXiv*, 2023.

[6] H. Li, Z. Wang, X. Mu, Z. Pan, and Y. Liu, "Near-field integrated sensing, positioning, and communication: A downlink and uplink framework," *arXiv*, 2023.

[7] D. Tse and P. Viswanath, *Fundamentals of Wireless Communication*. Cambridge University Press, 2005.

[8] Y. Zhang, X. Wu, and C. You, "Fast near-field beam training for extremely large-scale array," *IEEE Wireless Commun. Lett.*, vol. 11, no. 12, pp. 2625–2629, Dec. 2022.

[9] Z. He *et al.*, "Full-duplex communication for ISAC: Joint beamforming and power optimization," *IEEE J. Sel. Areas Commun.*, vol. 41, no. 9, pp. 2920–2936, Sept. 2023.

[10] M. Mohammadi, Z. Mobini, D. Galappaththige, and C. Tellambura, "A comprehensive survey on full-duplex communication: Current solutions, future trends, and open issues," *IEEE Commun. Surveys Tuts.*, pp. 1–1, 2023.

[11] D. Galappaththige, C. Tellambura, and A. Maaref, "Integrated sensing and backscatter communication," *IEEE Wireless Commun. Lett.*, vol. 12, no. 12, pp. 2043–2047, Dec. 2023.

[12] J. C. Bezdek and R. J. Hathaway, "Convergence of alternating optimization," *Neural, Parallel & Scientific Computations*, vol. 11, no. 4, pp. 351–368, Dec. 2003.

[13] S. Stanczak, *Fundamentals of Resource Allocation in Wireless Networks Theory and Algorithms*, 2nd ed. Berlin, Heidelberg: Springer Berlin Heidelberg, 2008.

[14] Q. Wu and R. Zhang, "Intelligent reflecting surface enhanced wireless network via joint active and passive beamforming," *IEEE Trans. Wireless Commun.*, vol. 18, no. 11, pp. 5394–5409, Nov. 2019.

[15] I. P'olik and T. Terlaky, *Interior Point Methods for Nonlinear Optimization*. Berlin, Germany; New York, NY, USA: Springer, 2010.

[16] F. Liu, C. Masouros, A. Li, H. Sun, and L. Hanzo, "MU-MIMO communications with MIMO radar: From co-existence to joint transmission," *IEEE Trans. Wireless Commun.*, vol. 17, no. 4, pp. 2755–2770, 2018.